

# FETI Method for Frequency-Domain Structural Dynamic Analyses Involving Localized Nonlinearities

Andrea Saponaro<sup>[0009-0000-8221-9222]</sup>,  
Giuseppe Battiato<sup>[0000-0001-7799-7775]</sup>,  
Christian M. Furrone<sup>[0000-0002-1817-7686]</sup>

## 1 Physical Problem, Discretization, and FETI Method

This section presents the physical problem, its discretization, and the Finite Element Tearing and Interconnecting (FETI) method. We consider a mechanical assembly of contacting bodies, whose finite element (FE) discretization of the elasticity problem yields the equilibrium equation:

$$\mathbf{M}\ddot{\mathbf{x}} + \mathbf{C}\dot{\mathbf{x}} + \mathbf{K}\mathbf{x} = \mathbf{f} - \mathbf{f}_{nl}(\dot{\mathbf{x}}, \ddot{\mathbf{x}}), \quad (1)$$

where  $\mathbf{M}, \mathbf{C}, \mathbf{K} \in \mathbb{R}^{n \times n}$  denote the mass, damping, and stiffness matrices, and  $\mathbf{x}, \mathbf{f}, \mathbf{f}_{nl} \in \mathbb{R}^n$  represent the displacement, external forces, and nonlinear contact forces, respectively. The matrices  $\mathbf{M}$  and  $\mathbf{K}$  are symmetric, with  $\mathbf{M}$  being positive definite and  $\mathbf{K}$  positive semidefinite. The damping matrix  $\mathbf{C}$  is defined as a linear combination of the two,  $\mathbf{C} = \alpha\mathbf{M} + \beta\mathbf{K}$ , and is therefore symmetric and positive semidefinite. Figure 1 (left) illustrates a simple assembly composed of two bodies.

Given a periodic excitation  $\mathbf{f}$ , the Harmonic Balance Method (HBM) is applied to Eq. (1) as described in [3]:

$$\mathbf{D}(\omega)\tilde{\mathbf{x}} - \tilde{\mathbf{f}} + \tilde{\mathbf{f}}_{nl}(\tilde{\mathbf{x}}) = \mathbf{0}, \quad \mathbf{D}(\omega) = \begin{bmatrix} -\omega^2\mathbf{M}_s + \mathbf{K}_s & -\omega\mathbf{C}_s \\ \omega\mathbf{C}_s & -\omega^2\mathbf{M}_s + \mathbf{K}_s \end{bmatrix}, \quad (2)$$

where  $\tilde{\mathbf{x}}, \tilde{\mathbf{f}}, \tilde{\mathbf{f}}_{nl}$  are the first-order Fourier coefficients of the displacement, excitation, and nonlinear forces, respectively. The nonlinear term  $\tilde{\mathbf{f}}_{nl}$  is computed using the Alternating Frequency/Time (AFT) method [2]. By decomposing the FE model into  $N$  domains — avoiding cutting planes coincident with contact areas [8] — and

---

Andrea Saponaro · Giuseppe Battiato · Christian M. Furrone  
Politecnico di Torino, Department of Mechanical and Aerospace Engineering, Italy, e-mail:  
andrea.saponaro@polito.it, giuseppe.battiato@polito.it, christian.furrone@polito.it

denoting the  $s^{\text{th}}$  domain by the subscript  $s$ , the FETI method is applied to Eq. (2) as described in [7, 8]:

$$\begin{cases} \mathbf{D}_s(\omega)\tilde{\mathbf{x}}_s - \tilde{\mathbf{f}}_s + \tilde{\mathbf{f}}_{nl,s}(\tilde{\mathbf{x}}) + \mathbf{B}_s^T \tilde{\boldsymbol{\lambda}} = \mathbf{0} & \forall s = 1 \dots N \\ \sum_{s=1}^N \mathbf{B}_s \tilde{\mathbf{x}}_s = \mathbf{0}, \end{cases} \quad (3)$$

where  $\mathbf{B}_s$  are the connectivity matrices (introduced as in [7]) and  $\tilde{\boldsymbol{\lambda}}$  are the Lagrange multipliers enforcing continuity across the interfaces. Figure 1 (right) illustrates the decomposition of a simple mechanical assembly. The residuals are defined as:

$$\begin{cases} \mathbf{r}_{L,s}(\tilde{\mathbf{x}}_s^k, \tilde{\boldsymbol{\lambda}}^k) = \mathbf{D}_s(\omega)\tilde{\mathbf{x}}_s^k - \tilde{\mathbf{f}}_s + \tilde{\mathbf{f}}_{nl,s}(\tilde{\mathbf{x}}^k) + \mathbf{B}_s^T \tilde{\boldsymbol{\lambda}}^k & \forall s = 1 \dots N \\ \mathbf{r}_B(\tilde{\mathbf{x}}_{1 \dots N}^k, \tilde{\boldsymbol{\lambda}}^k) = \sum_{s=1}^N \mathbf{B}_s \tilde{\mathbf{x}}_s^k. \end{cases} \quad (4)$$

Eq. (3) is linearized applying Newton Raphson (NR) leading to:

$$\begin{cases} \Delta \tilde{\mathbf{x}}_s^k = [\mathbf{D}_s(\omega) + \nabla \tilde{\mathbf{f}}_{nl}(\tilde{\mathbf{x}}_s^k)]^{-1} (-\mathbf{r}_{L,s}(\tilde{\mathbf{x}}_s^k, \tilde{\boldsymbol{\lambda}}^k) - \mathbf{B}_s^T \tilde{\boldsymbol{\lambda}}^k) & \forall s = 1 \dots N \\ \mathbf{F}_g^k \Delta \tilde{\boldsymbol{\lambda}}^k = \mathbf{d}^k, \end{cases} \quad (5)$$

with:

$$\mathbf{F}_g^k = -\sum_{s=1}^N \mathbf{B}_s [\mathbf{D}_s(\omega) + \nabla \tilde{\mathbf{f}}_{nl}(\tilde{\mathbf{x}}_s^k)]^{-1} \mathbf{B}_s^T, \quad (6)$$

$$\mathbf{d}^k = -\sum_{s=1}^N \mathbf{B}_s ([\mathbf{D}_s(\omega) + \nabla \tilde{\mathbf{f}}_{nl}(\tilde{\mathbf{x}}_s^k)]^{-1} \mathbf{r}_{L,s}(\tilde{\mathbf{x}}_s^k, \tilde{\boldsymbol{\lambda}}^k) - \tilde{\mathbf{x}}_s^k). \quad (7)$$

The interface problem (second equation in Eq. (5)) is solved iteratively, while the first equation in Eq. (5) is directly solved at domain level. The next section discusses the spectral properties of the matrix  $\mathbf{F}_g^k$ .



**Fig. 1** Mechanical assembly of two bodies in contact (left) and decomposition (right)

## 2 Spectral properties of the $F_g$ matrix

The objective of this section is to analyze the spectral properties of the  $F_g$  matrix, which influence the choice of the iterative method, its convergence, and the construction of an appropriate preconditioner introduced by deflation.

We begin by considering the generic  $s^{\text{th}}$  term of the summation in Eq. (6), evaluated at a given frequency  $\omega$  and at the  $k^{\text{th}}$  NR iteration:

$$F_{g,s}^k = B_s \left[ D(\omega) + \begin{bmatrix} \frac{\partial \Re(\tilde{f}_{nl}(\tilde{x}_s^k))}{\partial \Re(\tilde{x}_s^k)} & \frac{\partial \Re(\tilde{f}_{nl}(\tilde{x}_s^k))}{\partial \Im(\tilde{x}_s^k)} \\ \frac{\partial \Im(\tilde{f}_{nl}(\tilde{x}_s^k))}{\partial \Re(\tilde{x}_s^k)} & \frac{\partial \Im(\tilde{f}_{nl}(\tilde{x}_s^k))}{\partial \Im(\tilde{x}_s^k)} \end{bmatrix} \right]^{-1} B_s^T. \quad (8)$$

The term  $\nabla \tilde{f}_{nl}(\tilde{x}_s^k)$  represents the Jacobian of the contact forces (computed by the AFT procedure) and consists of four low-rank real symmetric blocks, different from one another. Assuming, for the moment, that the system operates in a linear regime (i.e., with a constant Jacobian), this Jacobian can be interpreted as an additional stiffness matrix  $K_{sa}$  added to  $K_s$ . Under this assumption, Eq. (8) becomes:

$$F_{g,s}^k = B_s \begin{bmatrix} -\omega^2 M_s + K_{sa} & -\omega C_s \\ \omega C_s & -\omega^2 M_s + K_{sa} \end{bmatrix}^{-1} B_s^T = B_s D_{sa}^{-1} B_s^T. \quad (9)$$

Furthermore, Eq. (9) can be rewritten as:

$$F_{g,s}^k = \begin{bmatrix} B_{\Gamma,s} & \mathbf{0} \\ \mathbf{0} & \mathbf{0} \end{bmatrix} \begin{bmatrix} D_{\Gamma\Gamma,sa} & D_{\Gamma O,sa} \\ D_{O\Gamma,sa} & D_{OO,sa} \end{bmatrix}^{-1} \begin{bmatrix} B_{\Gamma,s}^T & \mathbf{0} \\ \mathbf{0} & \mathbf{0} \end{bmatrix}, \quad (10)$$

where the subscripts  $\Gamma$  and  $O$  stand for interface nodes associated with Lagrange multipliers, and other nodes, respectively. Eq. (10) can be further written as:

$$\begin{bmatrix} B_{\Gamma,s} \left( D_{\Gamma\Gamma,sa} - D_{\Gamma O,sa} D_{OO,sa}^{-1} D_{O\Gamma,sa} \right)^{-1} B_{\Gamma,s}^T & \mathbf{0} \\ \mathbf{0} & \mathbf{0} \end{bmatrix} = \begin{bmatrix} B_{\Gamma,s} \mathcal{D}_{\Gamma\Gamma,s}^{-1} B_{\Gamma,s}^T & \mathbf{0} \\ \mathbf{0} & \mathbf{0} \end{bmatrix}, \quad (11)$$

where,  $\mathcal{D}_{\Gamma\Gamma,s}^{-1}$  is the Schur complement of the block  $D_{OO,sa}$  of the matrix  $D_{sa}$ .

The following theorems and lemmas are introduced to discuss the spectral properties of  $F_{g,s}^k$ . We define a matrix  $A \in \mathbb{R}^{m \times p}$  to be of the form  $\begin{bmatrix} S & -N \\ N & S \end{bmatrix}$ .

**Theorem 1** Given a non-singular matrix  $A \in \mathbb{R}^{(2n) \times (2n)}$  having the form defined above, with  $S, N \in \mathbb{R}^{n \times n}$  and  $S$  non-singular, its inverse has the same shape.

*Proof.* Let's start by considering a generic four block matrix:

$$\begin{bmatrix} S_1 & N_1 \\ N_2 & S_2 \end{bmatrix} \quad \text{with} \quad S_1, S_2, N_1, N_2 \in \mathbb{R}^{n \times n}. \quad (12)$$

It's inverse can be expressed as:

$$\begin{bmatrix} (\mathbf{S}_1 - \mathbf{N}_1 \mathbf{S}_2^{-1} \mathbf{N}_2)^{-1} & -\mathbf{S}_1^{-1} \mathbf{N}_1 (\mathbf{S}_2 - \mathbf{N}_2 \mathbf{S}_1^{-1} \mathbf{N}_1)^{-1} \\ -(\mathbf{S}_2 - \mathbf{N}_2 \mathbf{S}_1^{-1} \mathbf{N}_1)^{-1} \mathbf{N}_2 \mathbf{S}_1^{-1} & (\mathbf{S}_2 - \mathbf{N}_2 \mathbf{S}_1^{-1} \mathbf{N}_1)^{-1} \end{bmatrix}. \quad (13)$$

Using the Sherman-Morrison Woodbury formula it can be proved that:

$$-\mathbf{S}_1^{-1} \mathbf{N}_1 (\mathbf{S}_2 - \mathbf{N}_2 \mathbf{S}_1^{-1} \mathbf{N}_1)^{-1} = -(\mathbf{S}_1 - \mathbf{N}_1 \mathbf{S}_2^{-1} \mathbf{N}_2)^{-1} \mathbf{N}_1 \mathbf{S}_1^{-1}. \quad (14)$$

Posing  $\mathbf{S}_1 = \mathbf{S}_2 = \mathbf{S}$ ,  $\mathbf{N}_2 = -\mathbf{N}$  and  $\mathbf{N}_1 = \mathbf{N}$ :

$$\begin{bmatrix} \mathbf{S} & -\mathbf{N} \\ \mathbf{N} & \mathbf{S} \end{bmatrix}^{-1} = \begin{bmatrix} (\mathbf{S} + \mathbf{N} \mathbf{S}^{-1} \mathbf{N})^{-1} & -(\mathbf{S} + \mathbf{N} \mathbf{S}^{-1} \mathbf{N})^{-1} \mathbf{N} \mathbf{S}^{-1} \\ (\mathbf{S} + \mathbf{N} \mathbf{S}^{-1} \mathbf{N})^{-1} \mathbf{N} \mathbf{S}^{-1} & (\mathbf{S} + \mathbf{N} \mathbf{S}^{-1} \mathbf{N})^{-1} \end{bmatrix}. \quad (15)$$

□

**Lemma 1** Given a matrix  $\mathbf{A} \in \mathbb{R}^{(2n) \times (2n)}$  having the form defined above with  $\mathbf{S}, \mathbf{N} \in \mathbb{R}^{n \times n}$  and symmetric, let  $\text{spec}(\mathbf{A})$  denote the spectrum of  $\mathbf{A}$ . Then, the real and imaginary parts of the spectrum satisfy:  $\Re(\text{spec}(\mathbf{A})) \subseteq [\theta_{\min}(\mathbf{S}), \theta_{\max}(\mathbf{S})]$  and  $\Im(\text{spec}(\mathbf{A})) \subseteq [-|\theta(\mathbf{N})|_{\min}, |\theta(\mathbf{N})|_{\max}]$  where  $\theta(\mathbf{S})$  and  $\theta(\mathbf{N})$  are the eigenvalues of  $\mathbf{S}$  and  $\mathbf{N}$ , respectively.

*Proof.* The real part of the spectrum of  $\mathbf{A}$ ,  $\Re(\text{spec}(\mathbf{A}))$ , satisfies  $\Re(\text{spec}(\mathbf{A})) \subseteq [\theta_{\min}(\frac{\mathbf{A} + \mathbf{A}^T}{2}), \theta_{\max}(\frac{\mathbf{A} + \mathbf{A}^T}{2})] = [\theta_{\min}(\mathbf{S}), \theta_{\max}(\mathbf{S})]$ . Given  $\mu \in \text{spec}(\frac{\mathbf{A} - \mathbf{A}^T}{2})$ , and given  $\mu = \pm i\sigma$ ,  $\sigma \in \text{spec}(\mathbf{N})$  proving  $\Im(\text{spec}(\mathbf{A})) \subseteq [-|\theta(\mathbf{N})|_{\min}, |\theta(\mathbf{N})|_{\max}]$ .

□

**Lemma 2** The product of two matrices  $\mathbf{A} \in \mathbb{R}^{n \times n}$ , and the product of two matrices  $\mathbf{A}_1 \in \mathbb{R}^{m \times n}$  and  $\mathbf{A}_2 \in \mathbb{R}^{n \times n}$ , having the form defined above, preserves the shape.

*Proof.* Performing the products proves the lemma.

□

**Theorem 2** The matrix  $\mathcal{D}_{\Gamma, \mathbf{s}}^{-1}$  introduced in Eq. (11), has the shape of the previously defined matrix  $\mathbf{A}$ . The spectrum of  $\mathbf{F}_{\mathbf{g}, \mathbf{s}}^k$  can be approximated by the spectrum of  $\mathcal{D}_{\Gamma, \mathbf{s}}^{-1}$  if a non-redundant Lagrange multiplier scheme is used.

*Proof.* Since Eq. (11) is obtained by reordering Eq. (9) (which has the same shape as  $\mathbf{A}$ ), the square matrices  $\mathbf{D}_{\Gamma, \mathbf{s}a}$  and  $\mathbf{D}_{\mathbf{O}\mathbf{O}, \mathbf{s}a}$ , as well as the rectangular matrices  $\mathbf{D}_{\Gamma\mathbf{O}, \mathbf{s}a}$  and  $\mathbf{D}_{\mathbf{O}\Gamma, \mathbf{s}a}$ , all have the same shape as  $\mathbf{A}$ . By Theorem 1, the inverse  $\mathbf{D}_{\mathbf{O}\mathbf{O}, \mathbf{s}a}^{-1}$  also preserves this structure. Applying Lemma 2 then shows that the matrix  $\mathcal{D}_{\Gamma, \mathbf{s}} = \mathbf{D}_{\Gamma, \mathbf{s}a} - \mathbf{D}_{\Gamma\mathbf{O}, \mathbf{s}a} \mathbf{D}_{\mathbf{O}\mathbf{O}, \mathbf{s}a}^{-1} \mathbf{D}_{\mathbf{O}\Gamma, \mathbf{s}a}$  also retains the same structure. Finally, by applying Theorem 1 again, the inverse  $\mathcal{D}_{\Gamma, \mathbf{s}}^{-1}$  preserves this structure as well.

If a non-redundant Lagrange multipliers scheme is used, the spectrum of  $\mathbf{B}_{\Gamma, \mathbf{s}} \mathcal{D}_{\Gamma, \mathbf{s}}^{-1} \mathbf{B}_{\Gamma, \mathbf{s}}^T$  can be reasonably approximated by the spectrum of  $\mathcal{D}_{\Gamma, \mathbf{s}}^{-1}$  since the  $\mathbf{B}_{\Gamma, \mathbf{s}}$  matrices only introduces repeated eigenvalues.

□

From Eq. (9), and applying Lemma 1, the real part of the spectrum of the dynamic stiffness matrix  $\mathbf{D}_{sa}(\omega)$  is bounded by the eigenvalues of  $-\omega^2 \mathbf{M}_s + \mathbf{K}_{sa}$ , while the imaginary part is bounded by the spectrum of  $\omega \mathbf{C}_s$ . Since  $\mathbf{K}_{sa}$  is positive semidefinite and  $\mathbf{M}_s$  typically positive definite, the spectrum of  $(-\omega^2 \mathbf{M}_s + \mathbf{K}_{sa})^{-1}$  shifts toward the origin as  $\omega$  increases. The Schur complement  $\mathcal{D}_{\Gamma,s}^{-1}$  exhibits similar spectral behavior since its shape and structure is the same as  $\mathbf{D}_{sa}(\omega)$ , with its real spectrum increasingly centered around zero for larger  $\omega$ .

By Theorem 2, approximating the spectrum of  $\mathbf{F}_g$  as a combination of that of  $\mathbf{F}_{g,s}^k$ , it can be concluded that its distribution includes both positive and negative real part of eigenvalues, modulated by  $\omega$  as described above.

Although a linear region is assumed in the beginning, the Jacobian  $\nabla \tilde{f}_{nl}(\tilde{\mathbf{x}}_s^k)$  is low-rank affecting only DOFs at contact nodes (if present). Its spectral influence is thus negligible for the purposes of this work. Since  $\mathbf{F}_g^k$  is neither symmetric nor positive definite, the interface problem  $\mathbf{F}_g^k \tilde{\lambda}^k = \mathbf{d}^k$  is solved iteratively using GMRES.

### 3 Coarse space

The objective of this section is to introduce a new preconditioner based on deflation, to handle the spectral properties of the  $\mathbf{F}_g$  matrix. As commonly found in the literature [6, 1, 8], the following oblique projection matrix is introduced:

$$\mathbf{P}^k = \mathbf{I} - \mathbf{F}_g^k \mathbf{G} \left( \mathbf{G}^T \mathbf{F}_g^k \mathbf{G} \right)^{-1} \mathbf{G}^T, \quad (16)$$

where  $\mathbf{I}$  is the identity matrix and  $\mathbf{G} \in \mathbb{R}^{n \times m}$  the coarse space, having as columns the vectors to be deflated from  $\mathbf{F}_g$ . The deflated interface problems writes then as:

$$\begin{cases} \mathbf{P}^k \mathbf{F}_g^k \Delta \tilde{\lambda}_2^k = \mathbf{P}^k \mathbf{d}^k \\ \Delta \tilde{\lambda}^k = \Delta \tilde{\lambda}_2^k + \mathbf{F}_g^k \mathbf{G} \left( \mathbf{G}^T \mathbf{F}_g^k \mathbf{G} \right)^{-1} \mathbf{G}^T \left( \mathbf{d}^k - \mathbf{F}_g^k \Delta \tilde{\lambda}_2^k \right). \end{cases} \quad (17)$$

A common choice of  $\mathbf{G}$  starting from the idea of removing the zeros eigenvalues arising from the rigid body modes [6, 1, 8] of  $\mathbf{K}_s$  is:

$$\mathbf{G}_{RB} = [\mathbf{B}_1 \mathbf{R}_1 \cdots \mathbf{B}_{N_f} \mathbf{R}_{N_f}], \quad (18)$$

where  $\mathbf{R}_s \in \mathbb{R}^{n \times n}$  is the null space of the stiffness matrix  $\mathbf{K}_s$  of the  $s^{th}$  domain and  $N_f$  the number of floating domains (meaning with zero eigenvalues). This approach does not consider the effect of  $\omega$ , leading, as stated in Section 4 to a poor GMRES convergence. The proposed approach consists in introducing a coarse space  $\mathbf{G}_{FB} \in \mathbb{R}^{m \times p}$ , we called frequency based coarse space (FBCS), built using the spectrum of  $\mathcal{D}_{\Gamma,s}^{-1}$ , exploiting its properties presented in Section 2. Given:

$$\mathcal{D}_{\Gamma,s}^{-1} = \begin{bmatrix} \mathbf{S}_s & -\mathbf{N}_s \\ \mathbf{N}_s & \mathbf{S}_s \end{bmatrix}, \quad (19)$$

the eigenvalues of  $\mathbf{S}_s$  are computed and the eigenvectors associated to negative eigenvalues are stored as columns into  $\mathbf{R}_{FB,s}$ , leading to:

$$\mathbf{G}_{FB} = [\mathbf{B}_1 \mathbf{R}_{FB,1} \cdots \mathbf{B}_N \mathbf{R}_{FB,N}]. \quad (20)$$

From a physical standpoint, removing eigenvectors associated with negative eigenvalues eliminates non-physical solutions. To further improve convergence, eigenvectors corresponding to large eigenvalues are also discarded. Only the eigenvalues of  $\mathbf{S}_s$  are considered, as they typically dominate over those of  $\mathbf{N}_s$ , which mainly affect the imaginary part of the spectrum. The computational cost of the FBCS is comparable to that of the null-space approach, since both require the local computation of eigenvalues of similarly sized matrices. Problems dependent on a quadratic scalar parameter arise not only in structural dynamics [9] but also in wave propagation [5].

## 4 Numerical experiments

This section presents a numerical experiment to analyze the spectrum of the matrix  $\mathbf{F}_g$  and evaluate how the projection matrices  $\mathbf{P}_{RB}$  and  $\mathbf{P}_{FB}$  (built with  $\mathbf{G}_{RB}$  and  $\mathbf{G}_{FB}$ , respectively) influence the eigenvalue distribution and GMRES convergence. A FE model consisting of two bodies in contact (Fig. 2 A where contact area is highlighted by a violet plane) is used. The model has 2,916 DOFs, with 486 nonlinear contact DOFs, and uses a material with Young's modulus  $2 \times 10^{11}$  N/m<sup>2</sup>, density 7800 kg/m<sup>3</sup>, and Poisson's ratio 0.3. It is decomposed into 8 domains (Fig. 2 C).

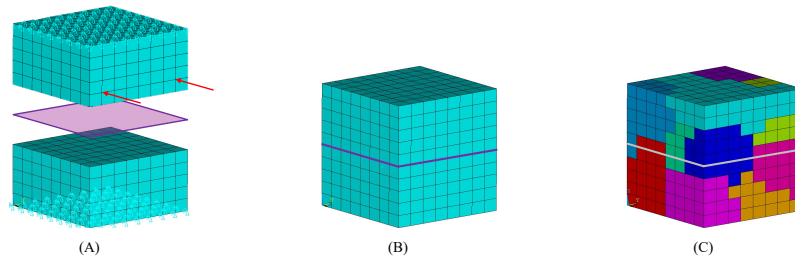


**Fig. 2** Cantilever bodies in contact between each others partitioned into 8 domains

To evaluate the effect of  $\mathbf{P}_{RB}$  and  $\mathbf{P}_{FB}$  on the  $\mathbf{F}_g$  spectrum and GMRES convergence, two frequencies — 50 Hz and 150 Hz — are chosen, corresponding to natural frequencies where resonance occurs (maximum response peak). Only the first NR iteration is considered, as it is the most critical for GMRES convergence due to the zero initial guess. Figure 3 (top) shows GMRES convergence (left) and spectra

(right) at 50 Hz. Without projection (red), negative eigenvalues cause stagnation, with convergence after 400 iterations. Using  $P_{RB}$  (green) deflates some negative eigenvalues, halving iterations to 200. The new coarse space  $P_{FB}$  (violet) deflates most negative and large eigenvalues, speeding convergence to 50 iterations. At 150 Hz (Fig. 3, bottom), the eigenvalue distribution shifts near zero, doubling GMRES iterations to 800 without projection.  $P_{RB}$  (green) is less effective, reducing iterations to 600. Meanwhile,  $P_{FB}$  (violet) maintains fast convergence (60 iterations), showing robustness against frequency changes. This proves how the presented coarse space efficiently addresses the effect of the parameter  $\omega$  on GMRES convergence.

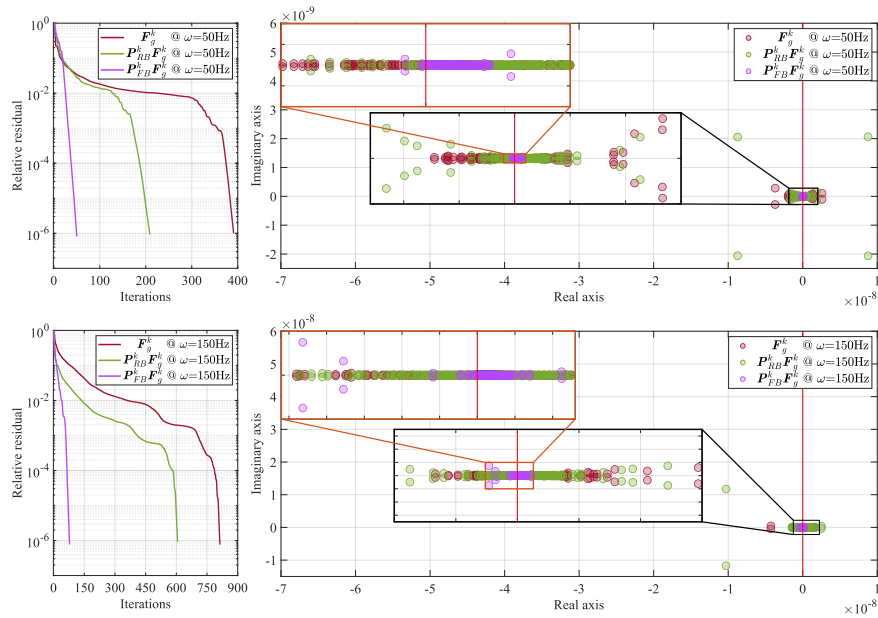


**Fig. 3** GMRES convergence and spectrum comparisons at  $\omega = 50$  Hz (top) and  $\omega = 150$  Hz (bottom) during the first NR iteration.

### 5 Conclusions

Using the FETI method to solve structural dynamics problems with localized nonlinearities enables studying larger FE models and overcomes limitations of traditional reduced order models [4] relying on physical assumption and being not always computationally feasible due to pre- and postprocessing steps. This approach involves solving an indefinite linear system with GMRES, which suffers from poor spectral properties due to its quadratic dependence on the parameter  $\omega^2$ . To address this, coarse spaces are introduced. The proposed frequency based coarse space effec-

tively mitigates the impact of  $\omega^2$ , improving GMRES convergence and altering the spectral properties of  $F_g$ , with similar computational cost to the rigid body modes coarse space.

**Acknowledgements** Ministry of University and Research (MUR), Italy as part of the HPC project from the MUR on PNRR funding program— Piano Nazionale di Ripresa e Resilienza, Mission 4 Component 2 Investment 1.4 (Grant Agreement No. CN00000013). We would like to acknowledge Professor Claudio Canuto (Politecnico di Torino) and Professor Valeria Simoncini (Università di Bologna) for their valuable discussions and insightful suggestions, which contributed to the development of some of the ideas presented in this work.

## References

1. Blahoš, J.: Parallel harmonic balance method for analysis of nonlinear mechanical systems. Ph.D. thesis, Imperial College London (2022)
2. Cameron, T.M., Griffin, J.H.: An alternating frequency/time domain method for calculating the steady-state response of nonlinear dynamic systems. *J. Appl. Mech.* **56**(1), 149–154 (1989)
3. Cardona, A., Coune, T., Lerusse, A., Geradin, M.: A multiharmonic method for nonlinear vibration analysis. *Int. J. Numer. Methods Eng.* **37**(9), 1593–1608 (1994)
4. Craig, R.R., Bampton, M.C.C.: Coupling of substructures for dynamic analyses. *AIAA J.* **6**(7), 1313–1319 (1968)
5. Farhat, C., Avery, P., Tezaur, R., Li, J.: Feti-dph: a dual-primal domain decomposition method for acoustic scattering. *J. Comput. Acoust.* **13**(3), 499–524 (2005)
6. Farhat, C., Chen, P.S., Mandel, J.: A scalable lagrange multiplier based domain decomposition method for time-dependent problems. *Int. J. Numer. Methods Eng.* **38**(22), 3831–3853 (1995)
7. Farhat, C., Roux, F.X.: A method of finite element tearing and interconnecting and its parallel solution algorithm. *Int. J. Numer. Methods Eng.* **32**(6), 1205–1227 (1991)
8. Saponaro, A., Battiato, G., Filippone, C.M., Zucca, S.: Parallel computation of the nonlinear forced response of a bladed disk with friction contacts using the feti method. *J. Eng. Gas Turbines Power* (2025)
9. Simoncini, V., Perotti, F.: On the numerical solution of  $(\lambda^2 a + \lambda b + c)x = b$  and application to structural dynamics. *SIAM J. Sci. Comput.* **23**(6), 1875–1897 (2002)